

Electronic structure and Jahn–Teller instabilities in a single vacancy in Ge

This article has been downloaded from IOPscience. Please scroll down to see the full text article.

2005 J. Phys.: Condens. Matter 17 L521

(<http://iopscience.iop.org/0953-8984/17/48/L02>)

View [the table of contents for this issue](#), or go to the [journal homepage](#) for more

Download details:

IP Address: 129.252.86.83

The article was downloaded on 28/05/2010 at 06:51

Please note that [terms and conditions apply](#).

LETTER TO THE EDITOR

Electronic structure and Jahn–Teller instabilities in a single vacancy in Ge

J Coutinho¹, R Jones², V J B Torres¹, M Barroso¹, S Öberg³ and P R Briddon⁴

¹ Department of Physics, University of Aveiro, Campus Santiago, 3810-193 Aveiro, Portugal

² School of Physics, University of Exeter, Exeter EX4 4QL, UK

³ Department of Mathematics, Luleå University of Technology, Luleå S-97187, Sweden

⁴ School of Natural Sciences, University of Newcastle upon Tyne, Newcastle upon Tyne NE1 7RU, UK

E-mail: coutinho@fis.ua.pt

Received 30 August 2005, in final form 20 October 2005

Published 11 November 2005

Online at stacks.iop.org/JPhysCM/17/L521

Abstract

Density functional modelling studies of the single vacancy in large Ge clusters are presented. We take a careful look at the origin of Jahn–Teller instabilities as a function of the vacancy net charge, resulting in a variety of structural relaxations. By comparing electron affinities of the vacancy with those from defects with well established gap states, we were able to estimate three acceptor states for the vacancy at $E(-/0) = E_v + 0.2$ eV, $E(=/-) = E_c - 0.5$ eV and $E(≡/=) = E_c - 0.3$ eV. As opposed to the Si vacancy, the defect in Ge is not a donor. We also show that these dissimilarities have fundamental consequences for the electronic/atomic picture of other centres, such as transition metals in germanium crystals.

Understanding the most elemental defects in semiconductors, vacancies (V) and self-interstitials (I), is a fundamental step in grasping the countless solid-state reactions that may occur during crystal growth, device processing and operation stages. Thanks to powerful spectroscopic techniques such as the electron paramagnetic resonance (EPR) approach, a detailed picture of the single vacancy in silicon has early emerged [1, 2], with important consequences for the understanding of many other fundamental and technological problems related to this material, such as self-diffusion, impurity diffusion, and the electronic structure of many centres such as transition metals.

Carrier mobility limitations in Si associated with a mostly probable replacement of SiO₂ as a gate dielectric with new high κ materials have led to serious consideration being given to the use of novel semiconductor materials for mainstream chip technology [3]. The main contenders are germanium and germanium rich silicon–germanium alloys.

In contrast to that for Si, the short spin–lattice relaxation time in Ge, together with the abundance of spin-9/2 ^{73}Ge species with large nuclear momentum, has hampered the detection of clear EPR defect signals. Consequently, a detailed picture of many elemental centres in Ge is still missing, and the single Ge vacancy is perhaps the most embarrassing case. Despite these difficulties, significant progress has been made by recent perturbed angular correlation spectroscopy (PACS) studies for Ge crystals, where, on the basis of the formation kinetics of ^{111}In –V pairs as a function of the Fermi level location, an $E(-/0) - E_{\text{v}} \sim 0.2$ eV acceptor state has been linked with the single vacancy [4]. The annealing temperature for V has also been estimated at ~ 200 K, and this was later confirmed by positron lifetime spectroscopy and x-ray diffraction [5, 6].

The success in modelling a Ge vacancy is also far from that attained in Si. Firstly, density functional theory, together with the local density approximation, predicts a nearly vanishing band gap for Ge when employing the invariably used supercell approach. This poses serious problems when modelling gap levels, as the calculated nearly metallic density of states of Ge overlaps all defect states. For instance, the vacancy–oxygen complex (VO) in Ge has an acceptor state at $E_{\text{v}} + 0.27$ eV [7], and local vibrational mode frequencies at 620 and 669 cm^{-1} were assigned to Ge–O–Ge units in VO^0 and VO^- [8, 9], respectively. Recent density functional supercell calculations [10] on the other hand give an acceptor state resonant with the conduction band, and the additional electron in VO^- actually falls in a conduction band state, resulting in a negligible difference between the vibrational frequencies of neutral and negatively charged centres. Secondly, it has been shown that Jahn–Teller driven reconstructions between vacancy *dangling bonds* produce long ranged strain fields which can only be accommodated by several hundreds of ligand atoms surrounding the defect [11, 12]. These strains span the characteristic length of computationally affordable supercells, resulting in spurious defect–defect interactions and, consequently, the predicted structures depend on the supercell size and shape, as well as on the scheme adopted for sampling the Brillouin zone [13]. These are among the reasons that make theoretical modelling reports on defects in Ge scarce. Early density functional modelling studies employing the Green’s function method [14] proposed five gap levels for the defect, corresponding to six stable charge states, from double positive (++) up to triple negative (\equiv). Unfortunately, these dealt with perfect unrelaxed vacancies only, and we know that a proper description of the Jahn–Teller distortions could well alter this picture. These distortions were recently investigated by means of density functional cluster calculations [15], but no electrical levels were reported. The fully relaxed supercell calculations by Fazio *et al* [16] predict (++)+, (+/0), (-/0) and (=/-) gap levels, and in line with the cluster calculations from [15], the resulting Jahn–Teller distortions were quantitatively smaller and qualitatively similar to those in the Si vacancy.

In this letter we present a close look at the atomic and electronic structure of the Ge vacancy by means of a spin density functional study using the AIMPRO code [17]. The pseudopotentials of Hartwigsen *et al* account for core electrons [18], and the local spin density approximation uses the Padé parametrization [19]. Valence states and the electron density are represented with the help of s, p, d-like Cartesian–Gaussian functions. We employ large hydrogen-terminated $\text{Ge}_{376}\text{H}_{196}$ spherical clusters with a vacant site at each centre, corresponding to a total of 28 shells of Ge ligand atoms. This approach has been successful in reproducing the measured electronic and structural details of the single-vacancy [11] and double-vacancy [12] centres in Si. Prior to defect studies, perfect clusters ($\text{Ge}_{377}\text{H}_{196}$) were fully relaxed, and under these conditions the lowest unoccupied Kohn–Sham state lies 2.17 eV above the highest occupied one. The large gap width is a consequence of surface confinement of the cluster states. All Ge–H surface units were then locked to their sites, a Ge atom was removed from the centre of the cluster and all remaining ligand atoms were freely allowed

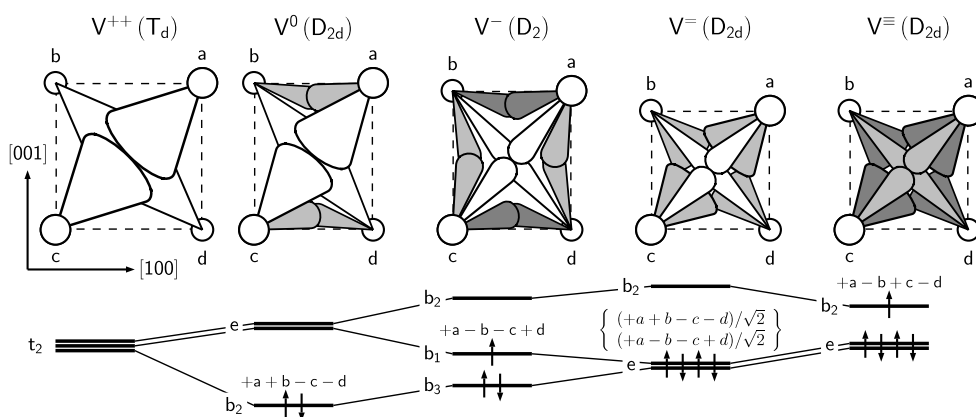


Figure 1. Scheme of the structural distortions in a Ge vacancy for several charge states of interest (up). Only low spin paramagnetic states are represented. The symmetry of each structure is shown within parentheses. Unoccupied, highest occupied and lower (fully occupied) levels are represented in white, light grey and dark grey bonds, respectively. The Jahn–Teller splitting pattern of the triplet (t_2) gap level is also shown (down), along with the symmetry representation of each level and the LCAO description of the highest occupied level.

to attain their equilibrium locations. Alternatively, the relaxation was constrained to a certain point group symmetry.

We are particularly interested in locating electrical levels. To do so, we adopt the *marker method* [20], where donor and acceptor states are calculated with respect to analogous levels from well established centres (marker defects). Hence, ionization energies (electron affinities) of the vacancy are compared to a similar calculation for the marker, and the difference is offset by the experimental donor (acceptor) level location of the latter. This method was shown to predict levels with an error bar of ~ 0.2 eV, but when the marker and the defect under scrutiny possess electron states which are similar in symmetry and extent, deviations from the measurements fall below 0.1 eV [21]. For donor markers, we have chosen substitutional sulfur ($E_c - E(0/+) = 0.28$ eV and $E_c - E(+/++) = 0.59$ eV) [22], selenium ($E_c - E(0/+) = 0.27$ eV and $E_c - E(+/++) = 0.51$ eV) [22], silver and gold ($E(0/+) - E_v = 0.035$ eV and $E(0/+) - E_v = 0.044$ eV, respectively) [23, 24]. For acceptor markers, substitutional silver ($E(-/0) - E_v = 0.116$ eV, $E_c - E(=/-) = 0.261$ eV and $E_c - E(\equiv/)=) = 0.113$ eV) [23], and substitutional gold ($E(-/0) - E_v = 0.135$ eV, $E_c - E(=/-) = 0.215$ eV and $E_c - E(\equiv/)=) = 0.056$ eV) [24], were adopted. The 4d and 5d shells on Au and Ag, respectively, were explicitly treated as valence states.

The removal of a Ge atom from the lattice produces four radicals located at the vertices of a perfect tetrahedron, labelled a , b , c and d in figure 1. Each radical may couple to their three neighbours, and within T_d symmetry they hybridize as a_1 and t_2 states. The singlet is resonant within the valence band, whereas the triplet is located within the gap. Analogously to the Si vacancy [1], the doubly positive vacancy in Ge (V^{++}) has an empty t_2 gap state, and is perfectly tetrahedral. Let us consider a simple linear combination of atomic orbitals (LCAO) arising from a , b , c and d dangling bonds (see V^{++} in figure 1). The triplet state components are $t_{2x} = +a - b - c + d$, $t_{2y} = +a - b + c - d$, and $t_{2z} = +a + b - c - d$ [1]. When this is partially occupied, electron–phonon coupling drives an Jahn–Teller distortion when the relaxation energy exceeds the exchange–coupling energy, in which case the occupancy follows Hund’s rule. Jahn–Teller distortions were investigated for charge states between

Table 1. Symmetry (Symm.), spin state (S), ab , ac atomic distances (according to figure 1), relative volume change ($100 \times \Delta v/v_0$) with respect to the volume of a perfect vacancy ($v_0 = 7.3662 \text{ \AA}^3$ with $ab = ac = 3.9686 \text{ \AA}$), and Jahn–Teller relaxation energies (E_{JT}) for the Ge vacancy in several charge states. All distances and energies are given in \AA and eV, respectively. The lattice constant for all calculations, $a_0 = 5.6125 \text{ \AA}$, was obtained from a volumetric relaxation of a Ge unit cell using periodic boundary conditions.

| | V ⁺⁺ | V ⁺ | V ⁰ | V [−] | V ⁼ | V [≡] |
|---------------------------|-----------------|-----------------|-----------------|----------------|-----------------|-----------------|
| Symm. | T _d | D _{2d} | D _{2d} | D ₂ | D _{2d} | D _{2d} |
| S | 0 | 1/2 | 0 | 1/2 | 0 | 1/2 |
| ab | 4.0056 | 3.7107 | 3.3008 | 3.2684 | 3.2596 | 3.2083 |
| ac | 4.0056 | 3.8519 | 3.7038 | 3.6189 | 3.5401 | 3.3789 |
| ac/ab | 1.0000 | 1.0381 | 1.1221 | 1.1072 | 1.0860 | 1.0532 |
| $100 \times \Delta v/v_0$ | 2.82 | −12.1 | −29.1 | −34.4 | −40.8 | −44.7 |
| E_{JT} | — | 0.06 | 0.10 | 0.00 | 0.11 | 0.04 |

++ (double positive) and ≡ (triple negative), by comparing the energy of atom- and spin-relaxed tetrahedral vacancies with similar calculations after trigonal (D_{3d}, C_{3v}, C₃), tetragonal (D_{2d} and S₄), orthorhombic (D₂, C_{2v}), monoclinic (C₂, C_{1h}) and triclinic (C₁) distortions. The D_{3d} structure is made up of two semi-vacancies that result on placing a Ge at the inversion centre of a perfect divacancy [13]. It is noteworthy that the local density approximation (LDA) treatment for the exchange–correlation energy tends to favour high spin states, and hence to underestimate Jahn–Teller distortion energies. However, in the limit of strong distortions (like for vacancy centres in Si) we expect to obtain the right symmetry and distortion directions, as well as the right order of magnitude for the energies. For example, local density cluster calculations of the Si divacancy give $E_{JT} = 0.10$ and 0.15 eV for V₂⁺ and V₂[−], respectively [15]. These are far away from the early results 1.3 and 2.4 eV from EPR data [25], but are close to the most recent estimates of 0.16 and 0.54 eV, respectively [26].

Structural details of fully relaxed vacancies in several charge states are shown in table 1. Charge states ++, +, 0, −, = and ≡ occur with T_d, D_{2d}, D_{2d}, D₂ (or T_d), D_{2d} and D_{2d} point group symmetries, respectively. These results are at variance with previous calculations [15, 16], which proposed C_{2v} symmetry for the negatively charged states. Our disagreement with [15, 16] is justified after looking more closely at each individual state. The V⁺⁺ (t₂ state is empty) has tetrahedral symmetry, showing a minute ($\Delta v/v_0 \sim 0.03$) volume increase with respect to the unrelaxed vacancy volume v_0 (table 1). When one or two electrons are added (+ and 0 charge states), the t₂ state splits through D_{2d} distortion into a half-occupied or fully occupied b₂ state, respectively, lying below an empty doublet state. Figure 1 shows that for the neutral vacancy $b_2 = +a + b - c - d$, which is a bonding state between ab and cd atom pairs. Its single and double occupancies lead to a structure with [001] axial symmetry, corresponding to Jahn–Teller relaxation energies (E_{JT}) of 0.06 and 0.10 eV when compared to tetrahedral relaxed V⁺ and V⁰ with $S = 1/2$ and 1 states, respectively. These are in line with previous calculations (0.02 and 0.12 eV for V⁺ and V⁰ [15]), and of the same order of magnitude as those estimated for the Si vacancy (0.05 and 0.32 eV for V⁺ and V⁰ [11]). Table 1 shows that each electron on the b₂ state produces a ~16% volume shrinkage, and the bond length anisotropy fraction (ac/ab) tells us that V⁺ and V⁰ are compressive along [001] and tensile along [100] and [010], respectively.

For the negative charge state we investigated several atomic/electronic configurations, of which we emphasize (i) C_{2v} and (ii) D₂ low spin states ($S = 1/2$) resulting from further Jahn–Teller splitting of the e state in V⁰, as well as (iii) a high spin state (t₂^{↑↑↑}) with T_d symmetry and $S = 3/2$. Other structures were tested, and they turned out to be unstable or energetically

Table 2. Donor and acceptor levels (eV) for the Ge vacancy. Calculations employ S, Se, Ag and Au marker impurities (see the text).

| Marker | S _s | Se _s | Ag _s | Au _s |
|---------|----------------|-----------------|-----------------|-----------------|
| V(+/++) | $E_c - 0.97$ | $E_c - 0.91$ | | |
| V(0/+) | $E_c - 0.95$ | $E_c - 0.98$ | $E_v - 0.11$ | $E_v - 0.12$ |
| V(-/0) | | | $E_v + 0.20$ | $E_v + 0.17$ |
| V(=/-) | | | $E_c - 0.50$ | $E_c - 0.54$ |
| V(≡/=) | | | $E_c - 0.25$ | $E_c - 0.27$ |

Au:[Xe].4f¹⁴.5d¹⁰.6s¹ have their d states lying within the valence density of states, leaving their 5s and 6s electrons resonating with the vacancy triplet state. This means that substitutional Au_s^q and Ag_s^q defects, where $q = 1, 0, -1, \dots$ stands for their charge states $+, 0, -, \dots$, show similar Jahn–Teller distortions to those found for V^(q-1). Curiously, ground states of Au_s⁰ and Ag_s⁰ are spin-1/2 with D₂ symmetry, and hence they adopt the configuration of V⁻ with low spin. The spin-3/2 Au_s⁰ and Ag_s⁰ centres are metastable by 0.05 eV. We also note that Au_s⁼ and Ag_s⁼ have perfect tetrahedral symmetry as their t₂⁰ states are fully occupied. Applying the above-mentioned procedure, we found that I_V(0/+) exceeds I_{Ag}(0/+) and I_{Au}(0/+) by 0.14 and 0.16 eV, placing the V(0/+) at E_v - 0.11 eV and E_v - 0.12 eV, respectively, and again ruling out any donor state for the vacancy.

Acceptor states were looked at by using Ag_s and Au_s acceptor markers. Now we use electron affinities A, i.e., for the vacancy we have A_V(-/0) = E(V⁻) - E(V⁰) = -3.29 eV, while for Ag_s and Au_s we obtain A_{Ag}(-/0) = -3.37 eV and A_{Au}(-/0) = -3.32 eV, respectively. This places the V(-/0) state 0.08 and 0.03 eV above Ag_s(-/0) and Au_s(-/0) acceptor levels, or at E_v + 0.20 eV and E_v + 0.17 eV, respectively, matching the location that has been estimated from the PACS measurements [4]. A similar procedure has been applied for second and third acceptor states (see table 2). Using second and third electron affinities of V, Au_s and Ag_s defects we find V(=/-) and V(≡/=) levels at around E_c - 0.50 eV and E_c - 0.25 eV, respectively. The ~0.7 eV band gap of Ge implies that the V(=/-) state falls very close to the V(-/0) level, and we cannot rule out a negative-U correlation energy between them. This effect is a consequence of the strong structural relaxation of V⁰ and V⁼ when compared to V⁻. Note that each electron on the t₂ split-off components shrinks the vacancy volume by ~16 and ~11% for V⁰ and V⁼, respectively. Therefore we have to admit that the E_v + 0.2 eV level that has been inferred from PACS measurements [4] could actually be assigned to a (0/=) occupancy state. Finally, the fact that Ag_s and Au_s defects lead to vacancy levels which differ by at most 0.04 eV implies that this would be the resulting error of a calculation utilizing the Ag_s marker to evaluate the Au_s levels.

We would like to acknowledge INTAS (grant No 03-50-4529), and the FCT in Portugal for financial support.

References

- [1] Watkins G D 1996 *Deep Centers in Semiconductors* 2nd edn, ed S T Pantelides (Switzerland: Gordon and Breach) p 177
- [2] Baraff G A, Kane E O and Schlüter M 1980 *Phys. Rev. B* **21** 5662
- [3] Chui O C, Gopalakrishnan K, Griffin P B, Plummer J D and Saraswat K C 2003 *Appl. Phys. Lett.* **83** 3275
- [4] Haesslein H, Sielemann R and Zistl C 1998 *Phys. Rev. Lett.* **80** 2626
- [5] Ehrhart P and Zillgen H 1990 *J. Appl. Phys.* **85** 3503
- [6] Polity A and Rudolf F 1999 *Phys. Rev. B* **59** 10025

-
- [7] Markevich V P, Hawkins I D, Peaker A R, Litvinov V V, Murin L I, Dobaczewski L and Lindström J L 2002 *Appl. Phys. Lett.* **81** 1821
- [8] Vanmeerbeek P and Clauws P 2001 *Phys. Rev. B* **64** 245201
- [9] Litvinov V V, Murin L I, Lindström J L, Markevich V P and Petuhg A N 2002 *Fiz. Tekh. Poluprov.* **36** 658
Litvinov V V, Murin L I, Lindström J L, Markevich V P and Petuhg A N 2002 *Semiconductors* **36** 621 (Engl. Transl.)
- [10] Coutinho J, Jones R, Briddon P R and Öberg S 2000 *Phys. Rev. B* **62** 10824
- [11] Ögüt S, Kim H and Chelikowsky J R 1997 *Phys. Rev. B* **56** R11353
- [12] Ögüt S and Chelikowsky J R 1999 *Phys. Rev. Lett.* **83** 3852
- [13] Puska M J, Pöykkö S, Pesola M and Nieminen R M 1998 *Phys. Rev. B* **58** 1318
- [14] Puska M J 1989 *J. Phys.: Condens. Matter* **1** 7347
- [15] Ögüt S and Chelikowsky J R 2001 *Phys. Rev. B* **64** 245206
- [16] Fazio A, Janotti A, da Silva A J R and Mota R 2000 *Phys. Rev. B* **61** R2401
- [17] Briddon P R and Jones R 2000 *Phys. Status Solidi b* **217** 131
- [18] Hartwigsen C, Goedecker S and Hutter J 1998 *Phys. Rev. B* **58** 3641
- [19] Goedecker S, Teter M and Hutter J 1996 *Phys. Rev. B* **54** 1703
- [20] Resende A, Jones R, Öberg S and Briddon P R 1999 *Phys. Rev. Lett.* **82** 2111
- [21] Coutinho J, Torres V J B, Jones R and Briddon P R 2003 *Phys. Rev. B* **67** 035205
- [22] Grimmeiss H G, Montelius L and Larsson K 1988 *Phys. Rev. B* **37** 6916
- [23] Huylebroeck G, Clauws P, Simoen E, Rotsaer E and Vennik J 1989 *Semicond. Sci. Technol.* **4** 529
- [24] Simoen E, Clauws P, Huylebroeck G and Vennik J 1987 *Semicond. Sci. Technol.* **2** 507
- [25] Watkins G D and Corbett J W 1965 *Phys. Rev.* **138** A543
- [26] Watkins G D 2005 *Proc. 23rd Int. Conf. on Defects in Semiconductors; Physica B* at press
- [27] Lento J, Pesola M, Mozos J-L and Nieminen R M 2000 *Appl. Phys. Lett.* **77** 232
- [28] Watkins G D 1983 *Physica B+C* **117/118** 9